Appl. Phys. B 70, 555–559 (2000) / Digital Object Identifier (DOI) 10.1007/s003400000200

Applied Physics B
Lasers
and Optics

Magneto-optical trap of metastable helium-3 atoms

M. Kumakura, N. Morita

Institute for Molecular Science, Myodaiji, Okazaki, 444-8585, Japan
(Fax: +81-564/55-4639, E-mail: kumakura@ims.ac.jp; morita@ims.ac.jp)

Received: 20 July 1999/Published online: 23 February 2000 –

Abstract. A magneto-optical trap of metastable ^{3}He atoms has been demonstrated. Some 10^5 atoms have been confined in a region with a diameter of ≈ 0.4 mm at a temperature of ≈ 0.5 mK; the atomic number density is estimated to be $\approx 10^9$ /cm^3 at the trap center. These characteristics of the ^{3}He trap are almost comparable to those of the ^{4}He trap so far demonstrated by many workers. By monitoring the fluorescence from the trap, the trap loss rate has also been measured and discussed.

PACS: 32.80.Pj; 34.50.Rk

In the past two decades, extensive developments have occurred in the laser cooling and trapping of neutral atoms, with many workers reporting the application of these techniques to such diverse atomic species as alkali atoms, alkali earth atoms, and rare gas atoms. For some of these atoms, the laser cooling and trapping of their different isotopic species have also been demonstrated, and have mainly applied to the study on isotopic differences in collision dynamics at ultralow temperatures [1–6]. Recent studies on Kr [3] and Xe [4, 5] atoms are typical examples of such studies, and they have investigated isotopic differences in Penning collisions of spin-polarized metastable atoms confined in their laser traps. In these studies, they have found that the rate coefficients of the Penning collisions between bosonic species are considerably larger than those between fermionic ones. More recently, the present authors have also carried out a similar study on spin-unpolarized metastable ^{3}He and ^{4}He atoms, and reported that, in contrast to the results on Kr and Xe, the Penning collision rate coefficient for ^{3}He (fermion) is in turn much larger than for ^{4}He (boson) [7].

In the above work on He atoms, a magneto-optical trap (MOT) [8] for ^{3}He has also been demonstrated for the first time, and this is the key technical achievement that has enabled our study on the isotopic difference in collisions of cold He atoms. In the case of such heavy atoms as Kr and Xe, since the mass difference among each isotopic species is very small, there are no significant differences in their (uncooled) initial velocities and laser-deceleration rates. Therefore, in general, all isotopic species can be laser-cooled and trapped with the same experimental setup. In fact, in the above studies on Kr and Xe, they have confined each isotopic species in its MOT by using the same apparatus; with only tuning the trap laser, every isotopic species has been trapped selectively. In the case of He atoms, however, since there is a relatively large mass difference between ^{3}He and ^{4}He, it is not very trivial whether the same experimental setup as has been used to achieve a MOT for ^{4}He by many authors [9–13] can be applied to a ^{3}He MOT as well. Moreover, the natural abundance of ^{3}He is so small that we have to make special efforts to trap a large number of ^{3}He atoms. The first demonstration of a ^{3}He MOT in our previous report [7] has been carried out in these contexts, and we have shown there that, in spite of the above problems, it is possible to confine a large number of ^{3}He atoms with only small modification in the conventional experimental setup for the ^{4}He MOT. In this report, however, only brief descriptions on the MOT itself have been presented, because our interest has been concentrated on the collision study. In the present paper, therefore, we would describe the detail of the experimental setup and procedure for our ^{3}He MOT. Since ^{3}He is a unique fermionic atom on account of its small mass and simple energy level structure, we can expect that such a ^{3}He MOT will be useful as a fundamental tool for future studies on the physics of fermions at ultralow temperatures.

1 Experimental

1.1 Laser cooling transitions

Like the case of ^{4}He, it is a metastable atom ^{3}He* (in the $2s\,^3S_1$ state) that can be laser-cooled and trapped. The energy level diagram relevant to the laser cooling of ^{3}He* atoms is shown in Fig. 1, along with the one for ^{4}He* for comparison. Although, unlike ^{4}He, the ^{3}He atom has hyperfine structure because of its nonzero nuclear spin (1/2), we can choose an ideal cooling transition $2s\,^3S_1$ ($F = 3/2, m_F = 3/2$) $\rightarrow 2p\,^3P_2$ ($F = 5/2, m_F = 5/2$), which is a cyclic transition quite analogous to the conventional cooling transi-

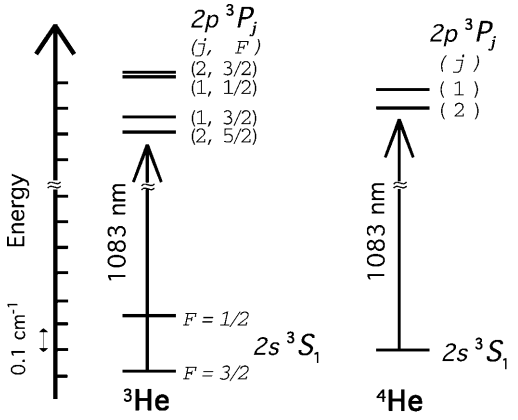

Fig. 1. Energy level diagrams relevant to the laser cooling and trapping of ^{3}He and ^{4}He atoms; each arrow shows the cooling transition for each isotope

tion $2s\,^3S_1\ (m=1) \rightarrow 2p\,^3P_2(m=2)$ for ^{4}He; although their transition wavelengths (≈ 1083 nm; photon momentum $\approx 6.1\times10^{-28}$ kg m/s) are slightly different, the difference between their transition electric dipole moments is negligible and radiative lifetimes of the upper states are both 97.85 ns (linewidth $\Gamma/(2\pi) \approx 1.6$ MHz; saturation intensity $I_{\rm sat} \approx 0.16\,{\rm mW/cm^2}$). Similarly, Zeeman shifts of these transitions are both linear, and their slopes with respect to magnetic field strength are the same (≈ 14 MHz/mT). However, the deceleration rate for ^{3}He*, which is estimated to be $6.3\times10^5\,{\rm m/s^2}$ under the full saturation condition, is considerably different from the one for ^{4}He* ($4.7\times10^5\,{\rm m/s^2}$ under the same condition) because of their mass difference.

1.2 Lasers

The laser system was just the same as was previously used for the ^{4}He* MOT [10]: infrared laser beams nearly resonant to the cooling transition were generated by two single-mode ring lasers employing LNA ($La_{1-x}Nd_xMgAl_{11}O_{19}$) crystals as gain media [14]. One laser was used for deceleration and confinement of ^{3}He* atoms, and the other was for optical collimation [15, 16] of a metastable ^{3}He* atomic beam, which will be described later. Their linewidths were both less than 0.5 MHz. By using discharge cells filled with pure ^{3}He gas, the frequency of each laser was locked at the saturation dip of the absorption spectrum of the cooling transition. Through Zeeman tuning of the absorption spectra, the two lasers were separately tuned to wavelengths suitable for their respective purposes.

1.3 Metastable ^{3}He beam*

In laser cooling of He atoms, their initial velocity is so large that we cannot sufficiently decelerate the atoms in a small cell; instead we have to decelerate them over a long distance by using an atomic beam. On the other hand, the natural abundance of ^{3}He is so small (1.4×10^{-4}%) that we cannot confine a large number of atoms by selective cooling of ^{3}He atoms contained in a natural He gas. Therefore in this experiment we use a ^{3}He gas sample of high purity (99.999%).

Metastable ^{3}He* atoms were produced by dc-discharge in pure ^{3}He gas cooled by pressure-reduced liquid nitrogen ($T \approx 40$ K) [16, 17]. The cold metastable atoms thus produced were injected into a vacuum chamber through a nozzle and skimmed off to make a metastable ^{3}He* atomic beam. This atomic beam was then optically collimated by irradiation with two orthogonal sets of red-detuned standing waves which transversely cross the atomic beam [15, 16]. The intensity and detuning of these laser beams were approximately $5\,{\rm mW/cm^2}$ and -3 MHz, respectively.

In such an experiment as uses a ^{3}He atomic beam, the heavy consumption of ^{3}He gas was a crucial problem on account of its high price. We therefore made use of an apparatus for purifying and recycling the used ^{3}He gas evacuated from the vacuum chamber. The intensity of the metastable beam was quite sensitive to the purity of the He gas, since atomic and molecular impurities significantly deexcited the He* atoms through collisional ionization processes. Therefore, to obtain an intense metastable beam, it was particularly important to remove the impurity as much as possible. The purification system consisted of an oil elimination filter, a bunch of cold channels, and molecular sieves cooled by liquid nitrogen; oil mist and dusts in the collected gas were eliminated by the filter, and the remaining oil mist and water were removed by the cold channels. Impurity gases, mainly consisting of nitrogen and oxygen, were eliminated by the molecular sieves, in which the gas pressure was kept at more than 2 bar in order to enhance the elimination efficiency for the impurity nitrogen gas. After all these purification processes, the collected gas was returned to the atomic beam source. With this system, more than 99.9% of the evacuated ^{3}He gas was collected and recycled without significant degradation of its purity, and consequently we could successfully maintain a constant intensity of the ^{3}He* atomic beam for a sufficiently long time.

The intensity of the metastable beam was measured by bombarding a stainless steel plate with the beam and detecting electrons ejected from its surface [18], and was found to be typically $10^{14}\,{\rm str^{-1}s^{-1}}$ after the optical collimation. The velocity distribution of the beam was obtained from a time-of-flight (TOF) measurement between the metastable beam source and a microchannel plate (MCP) detector placed 3.1 m

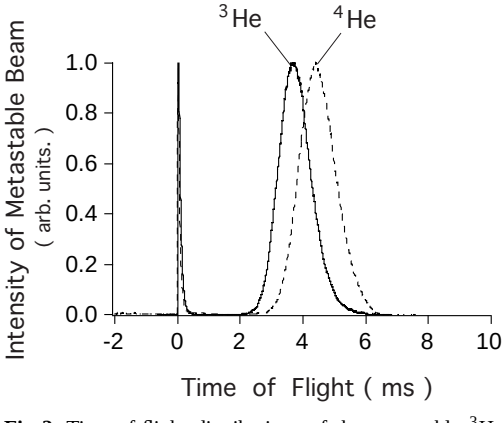

Fig. 2. Time-of-flight distributions of the metastable ^{3}He and ^{4}He atomic beams; the most probable velocities of the ^{3}He and ^{4}He beams are about 850 m/s and 710 m/s, respectively

downstream, with turning on the discharge in the beam source for a short time (0.1 ms). The TOF distribution thus measured is shown in Fig. 2 along with the one obtained for a ^{4}He* beam produced by the same beam source. The first sharp peak in the figure, which is due to XUV light generated by the discharge, indicates the zero flight time. From this measurement, we find that the most probable velocity of the ^{3}He* beam is approximately 850 m/s, whereas it is 710 m/s for the ^{4}He* beam. The ratio (≈ 1.2) between these velocities is approximately equal to the square root of the inverse mass ratio.

1.4 Deceleration and confinement

The metastable beam was optically decelerated by the conventional Zeeman tuning method [19], and then introduced to a 4 beam-type MOT [20]. The laser beam for the deceleration was one of the four laser beams forming the MOT [8, 20], and was softly focused on the nozzle of the metastable beam source. The tuning magnet, being about 1.5 m long, was the same one as used for the deceleration of ^{4}He* atoms [10]. However, in order to decelerate the ^{3}He* beam with an initial velocity 1.2 times larger than that of the ^{4}He* beam, we set the maximum field strength of the tuning magnet (≈ 65 mT) to be about 1.2 times larger than the one necessary for the deceleration of the ^{4}He* beam. Although, with this enhancement of the maximum field strength, the field gradient along the atomic beam was also increased by 1.2 times at every point along the beam, smooth and continuous deceleration of the ^{3}He* atoms was achieved owing to their deceleration rate $4/3$ times larger than that of ^{4}He*.

The experimental scheme of the 4-beam-type MOT was the same as was applied to the ^{4}He* MOT in our previous work [10]: it was composed of a quadrupole magnetic field and four laser beams directed toward the trap center in a tetrahedral configuration. All the four laser beams were circularly polarized, and their polarization directions were identical with respect to the direction of the magnetic field. The total intensity of the four laser beams was about 30 mW/cm^2 at the center of the MOT, and their detuning was -5 MHz. The quadrupole magnetic field was generated with an anti-Helmholtz coil pair placed along the axis of the atomic beam, and was continuously connected to the deceleration magnetic filed. The gradients of the magnetic field at the trap center were approximately 1.6 and 0.9 mT/cm along and across the atomic beam axis, respectively.

The total number and density distribution of ^{3}He* atoms confined in the MOT were measured by monitoring the fluorescence from the MOT with two calibrated near-infrared charge-coupled device cameras in the horizontal and vertical directions. The fluorescence intensity was also confirmed with a calibrated photodiode detector. From a calculation assuming the present laser intensity and detuning, the atomic population in the upper state of the cooling transition was estimated to be about 45% of the total population. From this estimation and the total fluorescence intensity measured, we obtained the total number of the confined atoms. The MOT images seen in both directions were well fitted to isotropic two-dimensional Gaussian distributions, so that the atomic number density distribution was approximated by an isotropic three-dimensional Gaussian distribution: $n(r) = n_0 \exp[-(r/r_0)^2]$. The MOT temperature was measured with a TOF method; after releasing the trapped atoms by turning off all four trap laser beams as well as all magnetic fields, we detected the atoms with an MCP detector placed 10 cm below the MOT center. From all these measurements, the total atomic number N, diameter $d\,(= 2\sqrt{\log 2}\, r_0)$, volume $V\,(= \pi^{3/2} r_0^3)$, peak density $n_0\,(= N/V)$, and temperature T of the MOT were found to be typically 10^5, 0.4 mm, 8×10^{-5} cm^3, 10^9 cm^{-3}, and 0.5 mK, respectively, at a background pressure of 3×10^{-7} Pa (5×10^{-8} Pa without a continuous flow of the atomic beam). All these characteristics were comparable to those of the ^{4}He* MOT so far demonstrated by the present authors [10] and other workers [9, 12, 13].

Here we should note that no "repumping" laser was used to achieve the above characteristics of the ^{3}He* MOT. In the case of ^{3}He* atoms, because of the presence of hyperfine structure, a certain fraction of the atomic population can escape into the $2s\,^3S_1$ ($F = 1/2$) state via $2p\,^3P_1$ ($F = 3/2$) through off-resonant optical pumping by the trap laser. In fact, in laser cooling and trapping of heavier atoms with hyperfine structure, it is usually required to use a repumping laser in addition to the trap laser in order to bring the escaping population back to the cooling transition. In the present case, however, the escape rate at our laser intensity and detuning was estimated to be as small as 1.1 s^{-1}, and this value was negligibly small compared with the rate of the trap loss (> 100 s^{-1}) caused by ionizing collisions at our MOT density, as will be shown in the next subsection. This fact allowed us to achieve the present MOT characteristics without any repumping laser. Such a small escape rate was due to the large splitting (1.8 GHz) between the $2p\,^3P_1$ ($F = 3/2$) and $2p\,^3P_2$ ($F = 5/2$) states, and was experimentally confirmed with a measurement of the trap loss rate, as will be described later.

1.5 Trap loss measurements

A metastable He* atom confined in the MOT collides not only with another He* atom but also with an atom or a molecule in the background gas. The He* atom has a high excitation energy of 19.8 eV above the ground state, and this excitation energy is large enough to ionize another He* atom as well as almost all atoms and molecules except He atoms in the ground state. In the MOT, therefore, two kinds of Penning ionization ($\mathrm{He}^* + \mathrm{He}^* \rightarrow \mathrm{He} + \mathrm{He}^+ + e^-$ and $\mathrm{He}^* + \mathrm{X} \rightarrow \mathrm{He} + \mathrm{X}^+ + e^-$, where X is an atom or a molecule in the background gas) and an associative ionization ($\mathrm{He}^* + \mathrm{He}^* \rightarrow \mathrm{He}_2^+ + e^-$) can occur and cause the trap loss. On the other hand, the trap loss is also caused by the heating through elastic collisions with atoms or molecules in the background gas at a room temperature. Moreover, in the case of ^{3}He*, the population escape should also, more or less, cause the trap loss. From these facts, the decay of the atomic density at each point of the MOT is described by the following rate equation:

$$\frac{\mathrm{d}n(r)}{\mathrm{d}t} = -\alpha_\mathrm{n} n(r) - \beta\{n(r)\}^2 \,, \tag{1}$$

where the coefficient α_n is the trap loss rate due to the heating, population escape, and ionizing collisions with the background gas, and β represents the trap loss caused by the ionizing collision between two He* atoms.

Assuming the density distribution to have an isotropic three-dimensional Gaussian profile, (1) is integrated with respect to r to give a rate equation for the total atomic number N:

$$\frac{\mathrm{d}N}{\mathrm{d}t} = -\alpha_{\mathrm{n}} N - \frac{\beta}{2\sqrt{2}V} N^2 \,. \tag{2}$$

Integrating (2), we finally obtain the time evolution of N:

$$N(t) = \frac{2\sqrt{2}\alpha_{\mathrm{n}} N(0) V}{\left[2\sqrt{2}\alpha_{\mathrm{n}} V + \beta N(0)\right] \exp(\alpha_{\mathrm{n}} t) - \beta N(0)} \,. \tag{3}$$

To determine α_{n} and β, the decay profile of $N(t)$ was experimentally measured by monitoring the fluorescence from the MOT: after steadily confining ^{3}He* atoms, the load of metastable atoms into the MOT was stopped at $t = 0$ by turning off the discharge in the metastable beam source, with keeping the trap laser on. The fluorescence decay after stopping the load was monitored by detecting a fraction of the fluorescence through a lens with a cooled-photomultiplier or a photodiode.

An example of the fluorescence decay profiles thus observed is shown in Fig. 3. As seen in this figure, the fluorescence decay is much faster than a simple exponential decay because of the ionizing collision between ^{3}He* atoms confined, and this behavior is well described by (3). By fitting (3) to the experimental decay profiles, the decay rates α_{n} and $\beta n_0(t = 0)$ are obtained for several values of $n_0(0)$, as shown in Fig. 4. From these results we finally obtain α_{n} and β, which are shown in Table 1. In this figure and table, we also show, for comparison, those obtained for ^{4}He* atoms confined in a MOT at the same temperature, background pressure, and detuning and intensity of the trap laser.

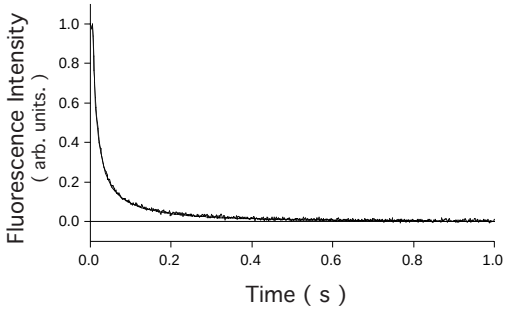

Fig. 3. Decay profiles of the fluorescence from the ^{3}He MOT; the *solid curve* is the one calculated from (3) fitted to the experimental decay profile

Table 1. The rate coefficients α_{n} and β experimentally determined

Isotope	Rate coefficients	
	$\alpha_{\mathrm{n}}/\mathrm{s}^{-1}$	$\beta/\mathrm{cm}^3\,\mathrm{s}^{-1}$
^{3}He	2.8 ± 0.2	$(8.9 \pm 1.8) \times 10^{-8}$
^{4}He	1.4 ± 0.1	$(4.8 \pm 1.0) \times 10^{-8}$

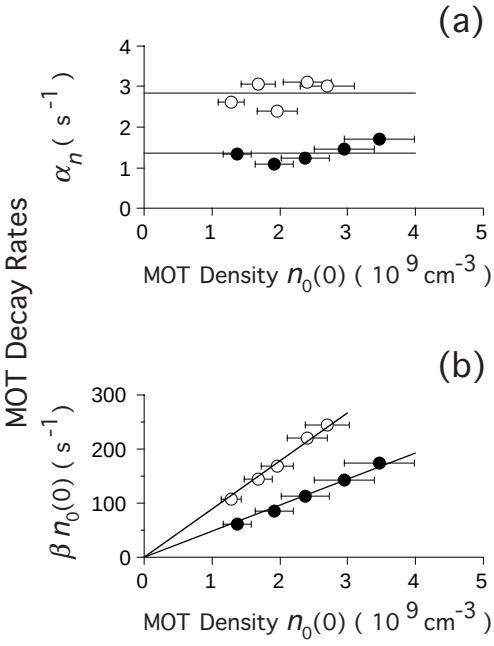

Fig. 4. Density dependences of the decay rates α_{n} and $\beta n_0(0)$; ○ and ● show experimental data obtained for the ^{3}He and ^{4}He MOTs at 0.5 mK, respectively. The *solid lines* are those fitted to the experimental data

2 Discussions

In the previous section we have shown that, with only two modifications in the conventional experimental setup and procedure for a ^{4}He* MOT, we can achieve a ^{3}He* MOT with almost the same characteristics as those of an ordinary ^{4}He* MOT: one modification is to add a recycling system for the expensive ^{3}He gas, and the other is a small increase in the magnetic field strength of the Zeeman tuning magnet. Although the smaller mass of the ^{3}He atom causes its larger initial velocity, it also results in a larger deceleration rate. The latter fact compensates the larger initial velocity to complete the deceleration in the same distance as is required for ^{4}He* atoms. This is the key reason why the same laser cooling apparatus as for ^{4}He* can be used for ^{3}He atoms in spite of their considerable mass difference.

As seen in Table 1, the linear loss rate α_{n} for ^{3}He* is larger than for ^{4}He* by $1.4\,\mathrm{s}^{-1}$. As is described in the previous section, there are two possible causes for the linear loss: collisions with the background gas and the population escape due to the off-resonant optical pumping. The former one should cause no significant difference in α_{n} between ^{3}He* and ^{4}He*, because their collision partners have kinetic energies at a room temperature and so the slight difference in the level structure between the two isotopes can hardly cause any appreciable difference in the collision rates. It is therefore reasonable to consider that the isotopic difference ($1.4\,\mathrm{s}^{-1}$) in α_{n} is due to the population escape. This difference is quite close to the value ($1.1\,\mathrm{s}^{-1}$) estimated for the population escape rate in the previous section. These results support our inference that, at the present MOT density, the population escape rate is negligibly small compared with the ionization loss rate βn_0 (≈ 100–$250\,\mathrm{s}^{-1}$) due to the collision between two ^{3}He* atoms. It is this fact that has allowed us to achieve the present characteristics of the ^{3}He* MOT without any re-

pumping laser, although at a much lower atomic density it would be necessary to use a repumping laser.

The rate coefficient β for ^{3}He* is also larger than for ^{4}He*. Unlike the case of α_n, the cause of this isotopic difference is not trivial, and its interpretation has briefly been reported in our previous paper [7] and will be described in detail elsewhere. Here we only point out that the rate coefficient β for ^{3}He* is not much larger than for ^{4}He*, and that this fact allows the ^{3}He* MOT to have a number density comparable to that of a ^{4}He* MOT under almost the same experimental conditions.

3 Conclusion

In this paper we have reported the detail of the experimental setup and procedure for a ^{3}He* MOT, which is demonstrated for the first time in our previous paper but is not described in detail there. We have shown that, in spite of the considerable mass difference between ^{3}He and ^{4}He and of the very small natural abundance of ^{3}He, it is possible to confine 10^5 ^{3}He* atoms in a MOT by using an experimental setup similar to the conventional one for a ^{4}He* MOT, and that the characteristics of the ^{3}He* MOT thus achieved are almost the same as those of an ordinary ^{4}He* MOT. Such a ^{3}He* MOT is quite useful not only for the study on the isotopic difference in cold collision dynamics, as is reported in our previous paper, but also, we believe, for the challenge to the Bose–Einstein condensation of fermionic atoms in the far future.

Acknowledgements. This work was partly supported by a Grant-in-Aid for Scientific Research from the Ministry of Education, Science, Sports, and Culture.

References

1. Z. Lin, K. Shimizu, M. Zhan, F. Shimizu, H. Takuma: Jpn. J. Appl. Phys. **30**, L1324 (1991)
2. F. Shimizu, K. Shimizu, H. Takuma: Phys. Rev. A **39**, R2758 (1989)
3. H. Katori, H. Kunugita, T. Ido: Phys. Rev. A **52**, R4324 (1995)
4. M. Walhout, U. Sterr, C. Orzel, M. Hoogerland, S.L. Rolston: Phys. Rev. Lett. **74**, 506 (1995)
5. C. Orzel, M. Walhout, U. Sterr, P.S. Julienne, S.L. Rolston: Phys. Rev. A **59**, 1926 (1999)
6. T. Kurosu, F. Shimizu: Jpn. J. Appl. Phys. **29**, L2127 (1990)
7. M. Kumakura, N. Morita: Phys. Rev. Lett. **82**, 2848 (1999)
8. E.L. Raab, M. Prentiss, A. Cable, S. Chu, D.E. Pritchard: Phys. Rev. Lett. **59**, 2631 (1987)
9. F. Bardou, O. Emile, J.-M. Courty, C.I. Westbrook, A. Aspect: Europhys. Lett. **20**, 681 (1992)
10. M. Kumakura, N. Morita: Jpn. J. Appl. Phys. **31**, L276 (1992)
11. J. Lawall, S. Kulin, B. Saubamea, N. Bigelow, M. Leduc, C. Cohen-Tannoudji: Phys. Rev. Lett. **75**, 4194 (1995)
12. W. Rooijakkers, W. Hogervorst, W. Vassen: Opt. Commun. **135**, 149 (1997)
13. H.C. Mastwijk, M. van Rijnbach, J.W. Thomsen, P. van der Straten, A. Niehaus: Eur. Phys. J. D **4**, 131 (1998)
14. L.D. Schearer, M. Leduc, D. Vivien, A-M. Lejus, J. Thery: IEEE J. Quantum Electron. **QE-22**, 713 (1986)
15. A. Aspect, N. Vansteenkiste, R. Kaiser, H. Haberland, M. Karrais: Chem. Phys. **145**, 307 (1990)
16. W. Rooijakkers, W. Hogervorst, W. Vassen: Opt. Commun. **123**, 321 (1996)
17. J. Kawanaka, M. Hagiuda, K. Shimizu, F. Shimizu, H. Takuma: Appl. Phys. B **56**, 21 (1993)
18. F.B. Dunning, A.C.H. Smith, R.F. Stebbings: J. Phys. B **4**, 1683 (1971)
19. W.D. Phillips, H. Metcalf: Phys. Rev. Lett. **48**, 596 (1982)
20. F. Shimizu, K. Shimizu, H. Takuma: Opt. Lett. **16**, 339 (1991)